ACS Medicinal Chemistry Letters

pubs.acs.org/acsmedchemlett Letter

Discovery of the First Orally Available, Selective $K_{Na}1.1$ Inhibitor: *In Vitro* and *In Vivo* Activity of an Oxadiazole Series

Andrew M. Griffin,* Kristopher M. Kahlig, Robert John Hatch, Zoë A. Hughes, Mark L. Chapman, Brett Antonio, Brian E. Marron, Marion Wittmann, and Gabriel Martinez-Botella

Cite This: *ACS Med. Chem. Lett.* 2021, 12, 593−602 Read Online

ACCESS | Metrics & More | Article Recommendations | Supporting Information

ABSTRACT: The gene *KCNT1* encodes the sodium-activated potassium channel $K_{Na}1.1$ (Slack, Slo2.2). Variants in the *KCNT1* gene induce a gain-of-function (GoF) phenotype in ionic currents and cause a spectrum of intractable neurological disorders in infants and children, including epilepsy of infancy with migrating focal seizures (EIMFS) and autosomal dominant nocturnal frontal lobe epilepsy (ADNFLE). Effective treatment options for *KCNT1*-related disease are absent, and novel therapies are urgently required. We describe the development of a novel class of oxadiazole $K_{Na}1.1$ inhibitors, leading to the discovery of compound **31** that reduced seizures and interictal spikes in a mouse model of *KCNT1* GoF.

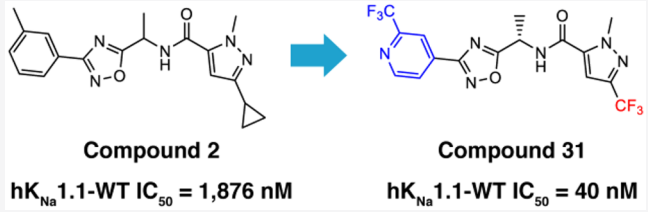

KEYWORDS: *Small molecule inhibitor, KCNT1 GoF mutations, HTS, oxadiazole series, SAR, DMPK, $K_{Na}1.1$*

KCNT1 encodes the neuronal potassium channel $K_{Na}1.1$ (Slack, Slo2.2) which is highly expressed throughout the central nervous system.[1] Like other voltage-gated potassium channels, functional $K_{Na}1.1$ channels are tetramers composed of four subunits. Each subunit contains a voltage sensing domain (S1−S4) and a pore-forming (S5-pore loop-S6) domain. However, $K_{Na}1.1$ is only weakly gated by voltage and is activated by alterations in cytoplasmic signaling cascades, energy state (ATP, NAD^+), and increases in intracellular sodium.[1] These features allow the channel to open in response to short-term increases in neuronal activity whereby increased potassium efflux would be thought to reduce neuronal activity. Paradoxically, disease-causing variants in *KCNT1* have invariably been found to increase the activity of the channel in a gain-of-function (GoF) manner. To date, orally active, selective inhibitors of $K_{Na}1.1$ have not been reported. Therefore, novel orally active inhibitors of $K_{Na}1.1$ would be important as potential therapeutics as well as tools to advance the understanding of the role of $K_{Na}1.1$ in neurophysiology.

The K_{Na} gene family contains both $K_{Na}1.1$ (Slack, Slo2.2; encoded by KCNT1) and $K_{Na}1.2$ (Slick, Slo2.1; encoded by KCNT2).[1] $K_{Na}1.1$ is thought to conduct a sodium-activated potassium current in various central and peripheral nervous system (CNS and PNS) networks, including both inhibitory and excitatory CNS networks. $K_{Na}1.2$ is thought to conduct the sodium-activated potassium current in the heart.[2] $K_{Na}1.1$ and $K_{Na}1.2$ have been suggested to form heterotetramers in cells that coexpress both genes.[1] However, association of $K_{Na}1.1$ and $K_{Na}1.2$ *in vivo* has not been demonstrated.

$K_{Na}1.1$ is thought to shape neural excitability on a subsecond time scale due to acute sensing of intracellular ionic and energy states.[3] K_{Na} channels have a large C-terminal region, which contains two regulators of K^+ conductance (RCK), which is where Na^+ binding is thought to occur.[1,4] Increases in intracellular Na^+ concentration associated with neuronal activity enhances $K_{Na}1.1$ channel activity and has been proposed to provide a vital feedback mechanism for controlling neural activity.[5] Previous work has also linked activation of $K_{Na}1.1$ to the presence of subthreshold I_{Na} (persistent I_{Na}) and enhancements in I_{Na} are well-known to cause neuronal hyperexcitability.[6] How variants in $K_{Na}1.1$ disrupt this regulation to produce a GoF phenotype is currently not well understood.[7,8] However, newly reported mouse models of *KCNT1* GoF will invariably provide new insights.[7,9,10]

KCNT1 channel mutants are located around three functional areas: the NAD^+ binding region situated in the C-terminus, the pore-forming region (between the S5 and S6 loops), and the RCK domains. All disease-causing variants are thought to be GoF and are associated with drug-resistant forms of infantile epilepsy such as the devastating epilepsy of infancy with migrating focal seizures (EIMFS)[3,11−13] or the less severe autosomal dominant nocturnal frontal lobe epilepsy (ADNFLE).[14−16] Less common epileptic disorders include West

Received: December 23, 2020
Accepted: March 1, 2021
Published: March 9, 2021

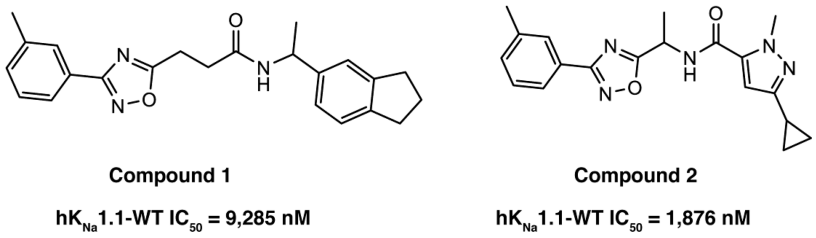

Figure 1. Oxadiazole HTS hits.

Scheme 1. Synthesis of Compound 3

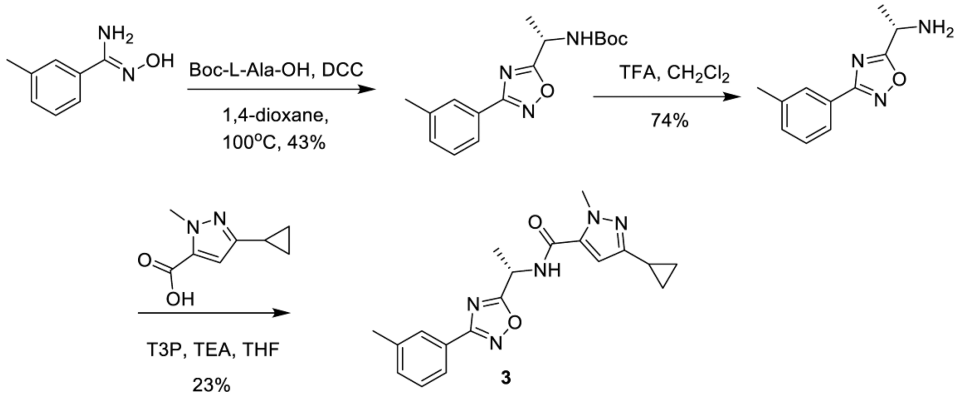

syndrome,[17] infantile spasm,[18] and Ohtahara syndrome.[19] Additional comorbidities are often present, including hypotonia, severe developmental delay, and movement disorder.[20]

Treatment options for *KCNT1*-related disease are extremely limited, and the seizures and comorbidities are intractable to conventional antiepileptics. Bepridil,[21,22] clofilium,[23] and quinidine[1,22−25] have been proposed as treatment options. However, because of nonspecificity in their mode of action[1,22,26] and recent questions around efficacy, their use is limited.[21,24,27] Currently, several groups have investigated agents that specifically inhibit $K_{Na}1.1$. Spitznagel et al. recently reported the discovery of VU0606170, a small molecule $K_{Na}1.1$ inhibitor with low micromolar potency.[5] VU0606170 was used to probe $K_{Na}1.1$ inhibition in neuronal cultures and proved useful at significantly reducing hyperexcitability in spontaneously firing cortical neuron cultures. Among other groups working on $K_{Na}1.1$ inhibitors, Cole et al. recently used the chicken $K_{Na}1.1$ cryo-EM structure to perform a virtual screen of 100,000 commercial compounds to find those that were predicted to bind in the channel pore.[22] A set of 17 compounds was selected from this exercise, of which 6 molecules were found to inhibit the $K_{Na}1.1$ channel with micromolar potency. Herein we describe our efforts in this area and describe for the first time *in vivo* activity of a small molecule $K_{Na}1.1$ inhibitor in a mouse model of *KCNT1* GoF.

A high throughput screen (HTS) using a rubidium (^{86}Rb) flux assay in HEK-TREX cells stably expressing the human EIMFS variant P924L (hK_{Na}1.1-P924L) was developed. Cells were preloaded with Rb and then incubated for 10 min with test compound in the presence of elevated KCl (5.4 mM) to depolarize the resting membrane potential and activate $K_{Na}1.1$ mediated Rb efflux. The amount of Rb efflux was quantitated and expressed as percent efflux. Approximately 72,000 compounds were screened using a custom-built library designed to maximize chemical diversity and obtained from several commercial suppliers. Screening was performed at 10 μM of compound and yielded an approximate 1% hit rate when defined as greater than 55% inhibition. These hits were reconfirmed for activity by screening in the same assay in a concentration response format where 270 of the hits were found to have a half maximal inhibitory concentration (IC_{50}) of 15 μM or less. The 270 compounds were subsequently tested in an automated, SyncroPatch patch clamp assay to refine the assessment of activity directly on $K_{Na}1.1$ current at physiological membrane potentials. HEK-TREX cells stably expressing human wildtype $K_{Na}1.1$ (hK_{Na}1.1-WT) were voltage clamped at −80 mV, and inhibition was measured using a voltage step to 0 mV. In this assay, $K_{Na}1.1$ was activated by increasing intracellular Na^+ to 70 mM. For the hKCNT1-WT and mKCNT1-WT assays, IC_{50s} were generated using concentrations ranging from 0.001 to 30 μM in half log steps and a minimum of three cells (replicates) per concentration (Tables 1−3). For compound **31**, all data represent a minimum of two (typically >3) independent experimental runs with at least five (typically >10) cells per concentration. Confirmed hits were subsequently clustered using chemoinformatic methods, and compound clusters were evaluated for their attractiveness to take forward into new analogue synthesis and development of structure−activity relationships (SARs). One cluster of interest, containing a phenyl oxadiazole scaffold, was selected for SAR studies and is described in this paper. Two such examples of oxadiazole[28] HTS hits are shown in Figure 1.

Compound **2** was of particular interest, and initial development of the scaffold sought to understand the basic SAR, as shown in Table 1. Compound **2** is a racemic mixture, and the individual enantiomers (compounds **3** and **4**) were synthesized in a chiral fashion according to the scheme outlined in Scheme 1. Coupling of *N*′-hydroxy-3-methylbenzimidamide with the corresponding protected amino acid gave the desired chiral oxadiazole intermediate, which was then deprotected and coupled to the pyrazole carboxylic acid to

https://doi.org/10.1021/acsmedchemlett.0c00675
ACS Med. Chem. Lett. 2021, 12, 593−602

Table 1. Initial SAR Exploration around HTS Hit

Compound	Structure	$hK_{Na}1.1$-WT IC_{50} (nM)
3	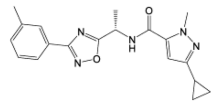	167
4	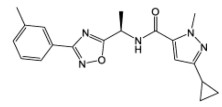	3,314
5	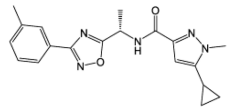	>30,000
6	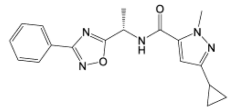	11,430
7	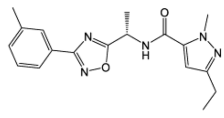	335
8	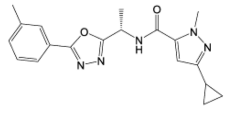	>30,000
9	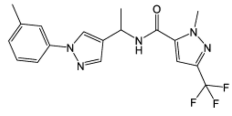	1,597
10	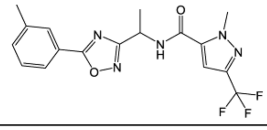	977
11	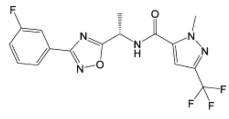	136
12	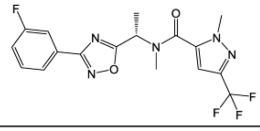	6,489
13	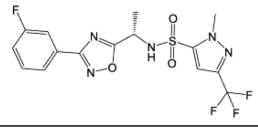	>30,000

afford compound **3**. All subsequent analogues were synthesized according to this general scheme.

Comparing the activity of compounds **3** and **4**, it was apparent that the stereochemistry of the methyl was important for inhibition at $K_{Na}1.1$, with the (*S*) isomer being the more active enantiomer. Not only is the stereochemistry important, but removal of the chiral methyl group led to greater than a 10-fold loss in activity (data not shown).

The pyrazole substitution pattern was found to be critical to activity. Comparing compound **5** to **3**, we found that moving the methyl to the alternative pyrazole nitrogen abolished activity. Removal of the methyl on the left-hand side aromatic ring (compound **6**) showed a significant loss of activity, although compound **11** demonstrates that fluorine is a suitable replacement for methyl (trifluoromethyl pyrazole has similar activity to cyclopropyl pyrazole). In an effort to establish if the

https://doi.org/10.1021/acsmedchemlett.0c00675
ACS Med. Chem. Lett. 2021, 12, 593−602

Table 2. Left Hand Side Heterocycle SAR

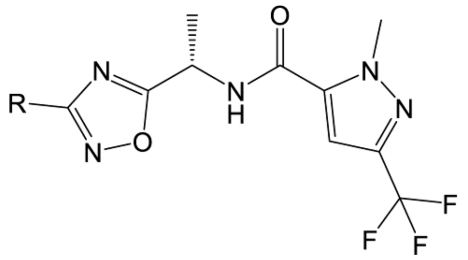

Compound	R	$hK_{Na}1.1$-WT IC_{50} (nM)
14	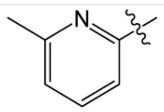	>30,000
15	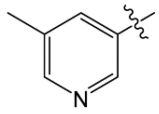	1,373
16	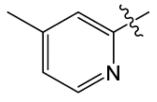	4,466
17	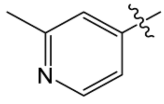	165
18	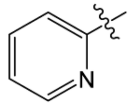	>30,000
19	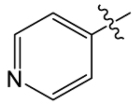	5,245
20	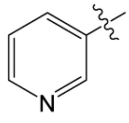	11,800
21	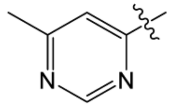	1,410
22	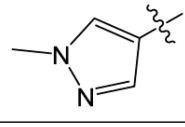	2,642

oxadiazole is simply a spacer to correctly orientate the other features of the molecules, we synthesized compounds **8**–**10** where alternative, readily accessible heterocycles were incorporated as replacements for the oxadiazole. All changes to the oxadiazole caused a reduction in activity, suggesting that electronic effects of the heterocycle may play a part in determining activity. Finally, compound **12** showed that *N*-methylation of the amide is not tolerated and compound **13** demonstrates that a sulfonamide cannot be used to replace the amide.

Our initial SAR scoping yielded molecules with high lipophilicity (measured $logD_{7.4}$ of 4 and higher), and we wished to establish if decreasing the lipophilicity was compatible with potent $K_{Na}1.1$ inhibition. We probed the

https://doi.org/10.1021/acsmedchemlett.0c00675
ACS Med. Chem. Lett. 2021, 12, 593−602

Table 3. Effects of Pyridine Substitution on Activity and Compound Properties

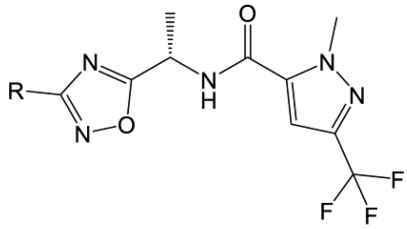

Compound	R	$hK_{Na}1.1$-WT IC_{50} (nM)	$mK_{Na}1.1$-WT IC_{50} (nM)	LogD	Kinetic Solubility (μM)	HCL_{int} (μL/min/mg)
17	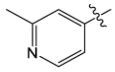	165	14,500	3.3	179	<9.6
23	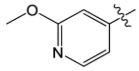	27	3,001	3.4	156	<9.6
24	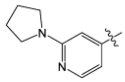	573		4.2	41	48
25	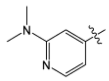	454		3.9	28	56
26	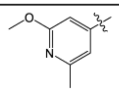	505		4.4	3	10
27	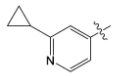	16	1,143	4.1	16	<9.6
28	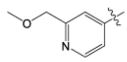	322	17,140	3.0	200	<9.6
29	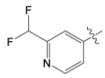	61	1,251	3.4	178	<9.6
30	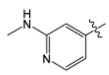	195	>30,000	3.4	143	28
31	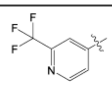	40	622	3.6	58	<9.6
32	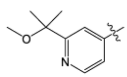	6,282		3.8	123	21
33	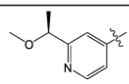	744				
34	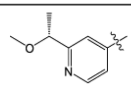	778				

introduction of various polar groups in the scaffold, with one such example being the use of heterocyclic rings in the left region as replacements for the existing substituted aromatic rings. The compounds in Table 2 describe the introduction of left-hand side heterocycles and their effect on $K_{Na}1.1$ inhibition. Compounds **18**−**20** contain unsubstituted pyridyl rings, and they were found to be poorly active, with the 4-pyridyl analogue, compound **19**, being the most active. However, in some cases, substitution on the pyridine ring did improve activity, with the 3-methyl substitution of the 4-pyridine (compound **17**) showing very promising $K_{Na}1.1$ inhibition with an IC_{50} of 165 nM. The same was not true for the 2-pyridines and 3-pyridine analogues which were significantly less active (compare compound **17** to **14**−**16**). Ring systems with additional heteroatoms such as compounds **21** and **22** were found to be weakly active.

https://doi.org/10.1021/acsmedchemlett.0c00675
ACS Med. Chem. Lett. 2021, 12, 593−602

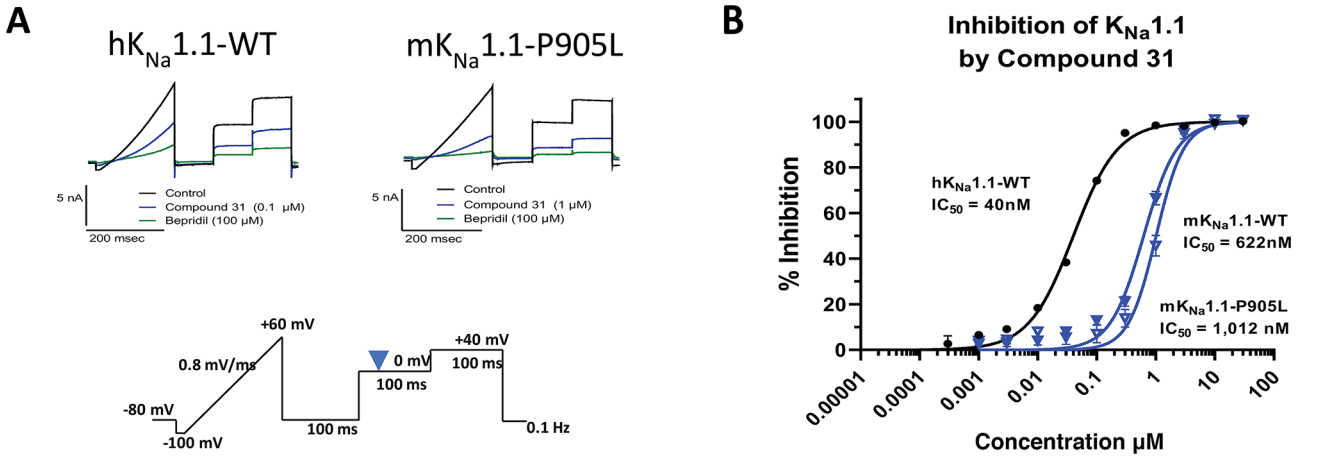

Figure 2. *In vitro* profile of compound **31** on human and mouse $K_{Na}1.1$.

The SAR of compound **17** was further probed by varying the substituents on the pyridine ring as shown in Table 3. Compound **17** showed good aqueous kinetic solubility and *in vitro* stability in human liver microsomes. Changing the methyl group of compound **17** to the *o*-methoxy group in compound **23** enhanced the activity and maintained good *in vitro* metabolic stability. Tertiary amines at the meta position have weaker activity and poorer metabolic stability as seen with compounds **24** and **25**. The secondary amine **30** did show comparable activity to compound **17** but was weaker than the methoxy analogue compound **23** as well as less metabolically stable (HCL_{int} of 28 μL/min/mg compared to <9.6 μL/min/mg).

Placing a pendent methyl ether at the meta position, as shown by compound **28**, caused a considerable loss in activity, which was also found with the substituted ether compounds **32**−**34**. Addition of a second substituent to the aromatic ring caused a greater than 10-fold drop in activity (compare compound **26** to **23**), and the cyclopropyl analogue **27** was found to be the most potent analogue in the series.

Where measured, it should be noted that all compounds showed a significant loss of activity at the mouse wildtype $K_{Na}1.1$ ($mK_{Na}1.1$-WT) channel compared to $hK_{Na}1.1$-WT (see Table 3). For example, our initial pyridine hit, compound **17**, had an IC_{50} of 165 nM at $hK_{Na}1.1$-WT but an IC_{50} of >14,000 nM at $mK_{Na}1.1$-WT. Given that our preclinical *in vivo* testing was performed in a mouse model of *KCNT1* GoF, an *in vivo* assessment of the series was technically challenging due to a drop-off with mouse activity. The reason for the marked difference in potency between human and mouse wildtype channels is not well understood. Fortunately, the trifluoromethyl pyridyl analogue **31**, although less active than some analogues at $hK_{Na}1.1$-WT (IC_{50} 40 nM), was found to be the most potent compound at $mK_{Na}1.1$-WT (IC_{50} 622 nM) with a modest 15-fold shift between the orthologues (Figure 2). Moreover, activity was retained at $mK_{Na}1.1$-P905L (25-fold shift, Figure 2), which represents the mouse ortholog containing the human P924L EIMFS variant. This retained activity facilitated *in vivo* testing. Based on the described SAR findings, compound **31** was selected as a candidate to characterize further in our *in vitro* and *in vivo* assays. Additional patch clamp based, primary pharmacology revealed IC_{50}'s of 49 nM for cynomolgus monkey $K_{Na}1.1$-WT and 545 nM for rat $K_{Na}1.1$-WT.

$K_{Na}1.1$ inhibition data described so far were determined using the human or mouse wildtype channels. Given that we aim to treat individuals with GoF $K_{Na}1.1$ variants, it is important to profile compounds of interest for activity across several variants due to their disparate locations in the channel protein. Cell lines stably expressing individual human *KCNT1* GoF variants were created to represent recurrent variants located across the channel structure: transmembrane domains, RCK1, and RCK2. The activity of compound **31** at these variants was assessed (Figure 3), and all variants were less

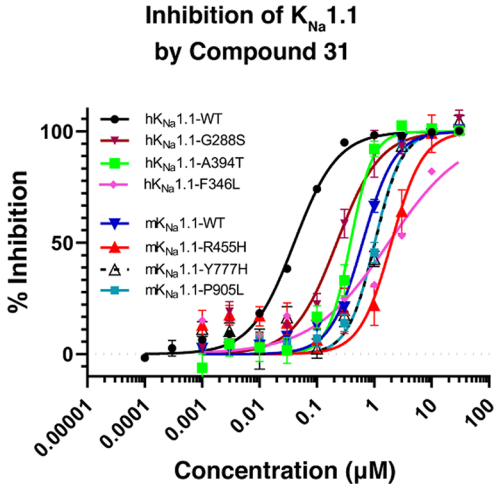

Figure 3. Effect of compound **31** on human and mouse $K_{Na}1.1$ variants.

active when compared to $hK_{Na}1.1$-WT with activity at the human variants ranging from 221 nM (G288S) to 1768 nM (F346L). Such a range of activities is a feature we have seen for several other members of the oxadiazole series (data not shown).

Further characterization of compound **31** included an assessment of potential secondary activity across a panel of 80 targets at 10 μM compound concentration, using binding displacement assays. Only two hits showed >50% activity: translocator protein (TSPO) (63% displacement) and $GABA_A$ Cl^- channel (74% displacement). Furthermore, using patch clamp analysis in a panel of ion channels, compound **31** showed no significant inhibition at hERG (IC_{50} 11.9 μM), $hNa_V1.5$ (IC_{50} 42 μM), $Ca_V1.2$ (IC_{50} 10.7 μM), or I_{Ks} (IC_{50}

https://doi.org/10.1021/acsmedchemlett.0c00675
ACS Med. Chem. Lett. 2021, 12, 593−602

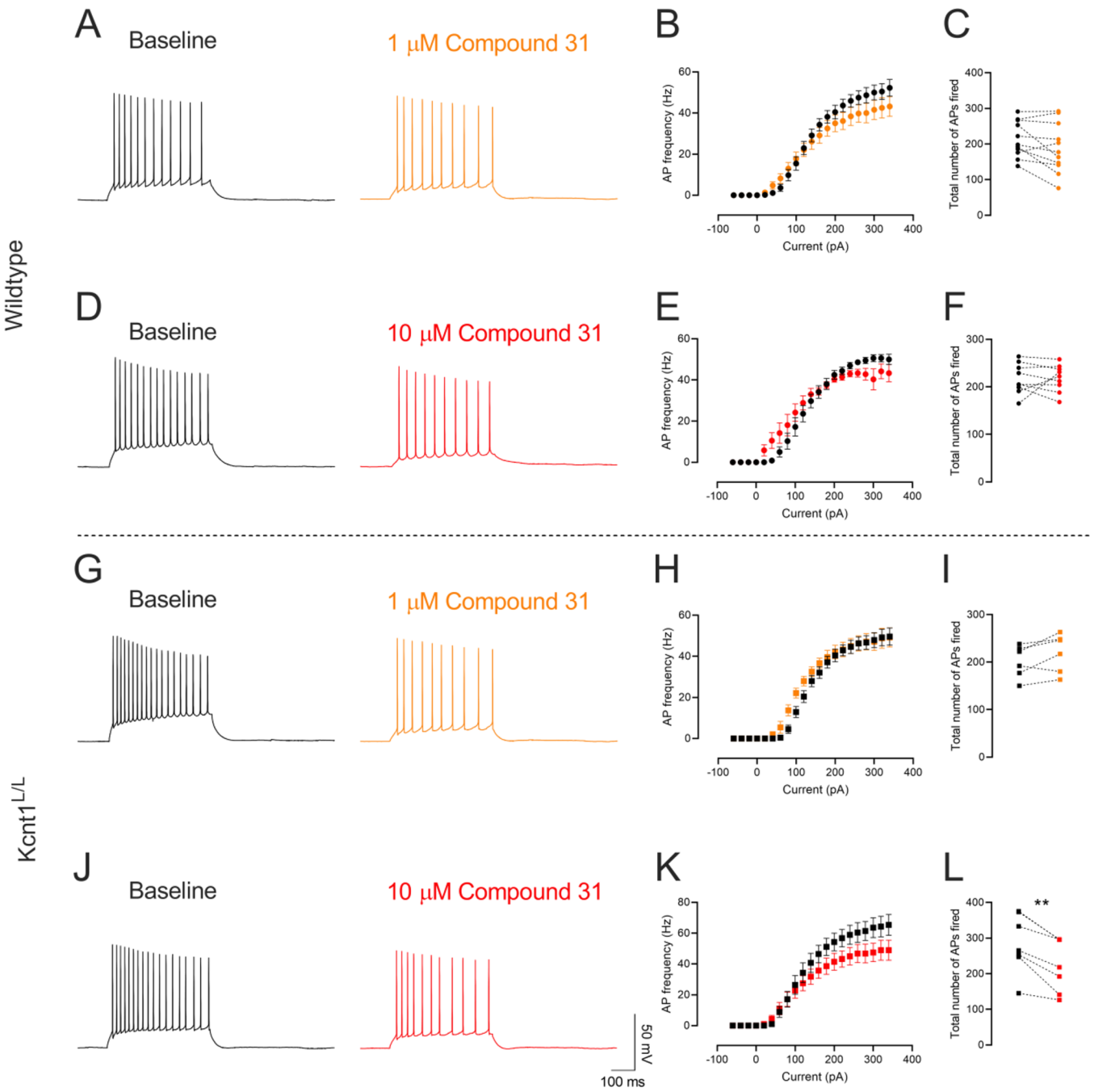

Figure 4. Effect of comnpound **31** on CA1 pyramidal neurons from wildtype and Kcnt1$^{L/L}$ mice. (A,D,G,J) Represenative traces of baseline (black) and in the presence of 1 μM (orange) and 10 μM (red) compound **31**. Quantification of (B,E,H,K) input-frequency relations and (C,F,I,L) total number of action potentials fired. Data presented as mean ± SEM and paired individual data points. **p < 0.01.

18.5 μM). Finally, additional patch clamp based assessment of compound **31** at the potassium channels BK (IC_{50} 13.2 μM) and K_{Na}1.2/Slick/KCNT2 (IC_{50} 16.4 μM) showed weak activity. This package of data indicates that compound **31** shows good overall selectivity for the K_{Na}1.1 channel.

The primary activity of compound **31** was further assessed in a native tissue brain slice preparation. Whole-cell patch clamp recordings from CA1 pyramidal neurons in acute mouse brain slices were performed. The effects of compound **31** on neuronal firing were evaluated in brain slices from WT mice and mice homozygous for mKcnt1-P905L (Kcnt1$^{L/L}$). The Kcnt1$^{L/L}$ mouse line recapitulates many key features of the human disease, including spontaneous seizures, high interictal spike frequency, and reduced survival.[10] In brain slices prepared from p16−30 day old WT or Kcnt1$^{L/L}$ mice, a current injection protocol was used to determine action potential firing at baseline and in the presence of 1 μM or 10 μM of compound **31**. In neurons from WT mice, there was a nonsignificant trend toward a decrease in the total number of action potentials fired in the presence of 1 μM (p = 0.054, baseline 213.5 ± 15.21, compound **31** 188.5 ± 21.09, n = 11 paired cells) and 10 μM compound **31** (p = 0.897, baseline 216.8 ± 10.65, compound **31** 218.1 ± 9.43, n = 9 paired cells) (Figure 4A−F). In neurons from Kcnt1$^{L/L}$ mice, although 1 μM compound **31** did not alter firing (p = 0.075, baseline 201.2 ± 13.00, compound **31** 219.5 ± 16.5, n = 6 paired cells),

https://doi.org/10.1021/acsmedchemlett.0c00675
ACS Med. Chem. Lett. 2021, 12, 593−602

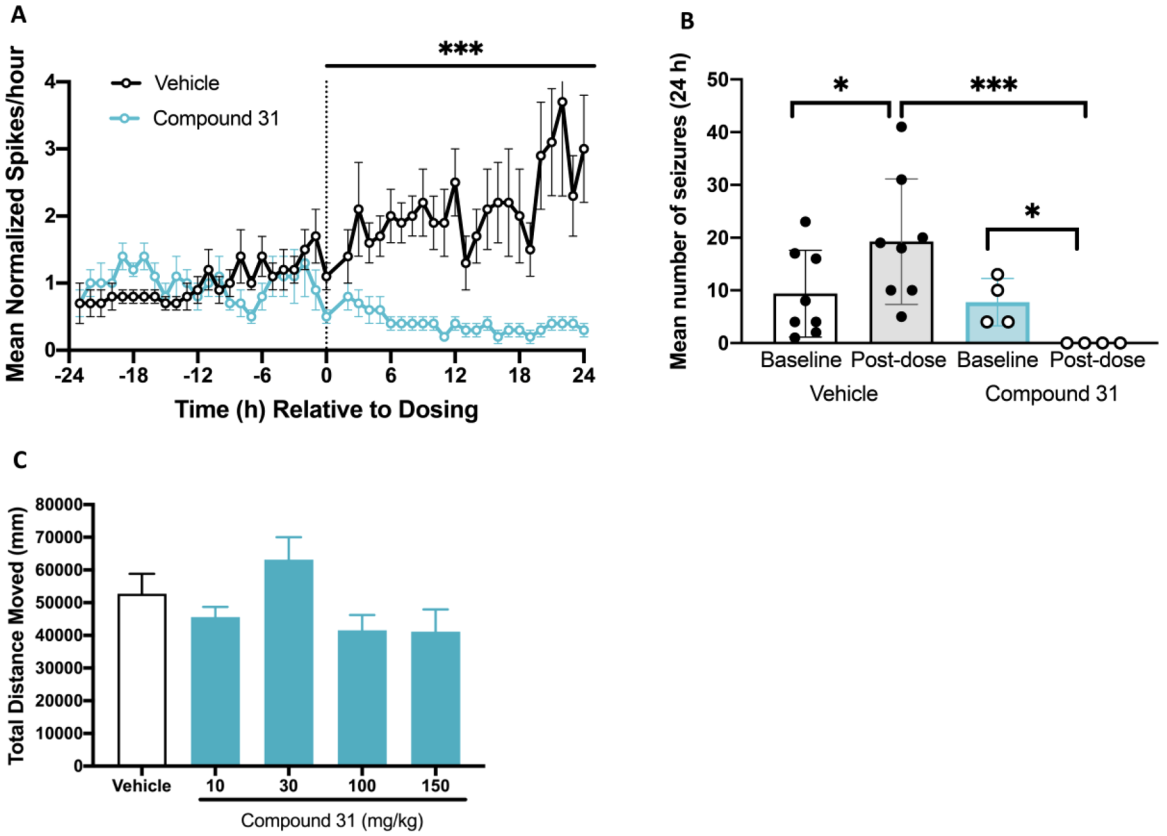

Figure 5. Compound **31** normalizes EEG phentotype in Kcnt1$^{L/L}$ mice without affecting spontaneous locomotor activity. Acute administration of compound **31** (30 mg/kg, SC) decreased interictal spike frequency (A) and decreased mean number of seizures (B) in Kcnt1$^{L/L}$ mice. Compound **31** (10−150 mg/kg) did not affect spontaneous locomotor activity in wildtype CD-1 mice (C). Data are mean ± SEM, n = 4−10; *P < 0.05 vs respective baseline; ***P < 0.0001 vs vehicle.

application of 10 μM compound **31** resulted in a significant reduction in firing (p = 0.0015, baseline 284.4 ± 31.10, compound **31** 223.4 ± 28.01, n = 7 paired cells) (Figure 4G−L).

Pharmacokinetics of compound **31** in CD-1 mice showed a compound with good brain penetration and low clearance, suitable for *in vivo* pharmacological testing. A 0.5 mg/kg IV dose (10% DMSO, 10% Solutol, and 80% water vehicle) had a clearance of 2.0 mL/min/kg, a Vd_{ss} of 1.88 L/kg, and a half-life of over 20 h. Upon oral dosing, compound **31** was fully bioavailable and, with an oral dose of 30 mg/kg, slightly more compound was present in the brain compared to plasma, with 98.3% compound binding to mouse plasma protein and 97.8% compound binding to mouse brain tissue.

Compound **31** was assessed *in vivo* in the Kcnt1$^{L/L}$ mouse model.[10] Kcnt1$^{L/L}$ mice (P32−40) were implanted with EEG electrodes to allow monitoring of electrographic seizure and interictal spike frequency. After collecting a 24 h recording to establish baseline interictal spike and seizure frequency, Kcnt1$^{L/L}$ mice were dosed with vehicle (10% DMSO, 10% Solutol, and 80% water vehicle) or compound **31** (30 mg/kg, SC) and EEG recordings collected for a further 24 h.

Figure 5A depicts mean normalized interictal spike frequency over time. After dosing with vehicle, mice continue to have rising interictal spike frequency, whereas after dosing with compound **31** (30 mg/kg, SC) there is a robust reduction in interictal spike frequency that persists over the 24 h period. A subset of Kcnt1$^{L/L}$ mice (n = 12) exhibited multiple seizures (average 8.8 ± 2.0 seizures/24 h) during the 24 h baseline period (Figure 5B). Not a single seizure was observed in the 24 h period after dosing with compound **31** (30 mg/kg, SC). At this dose of compound **31** (30 mg/kg, SC), the maximum free brain concentration is approximately 270 nM, which is in the region of a quarter of the *in vitro* IC_{50} (1012 nM) at $mK_{Na}1.1$-P905L. For ion channel modulators, achieving *in vivo* activity at free concentrations in the brain which are well below the IC_{50} determined using *in vitro* assays is not unprecedented. Indeed the sodium channel blocker carbamazepine shows anticonvulsant efficacy in mice with a free brain EC_{50} of ∼5.6 μM despite its potency for blocking peak sodium currents *in vitro* (IC_{50}) being 10−100-fold[29,30] higher (unpublished data). Similarly, the K_v7 potassium channel positive modulator retigabine is efficacious at free brain concentrations of around one-third of the *in vitro* EC_{50}.[30,31] To determine whether compound **31** had any nonspecific sedative effects, the molecule was assessed for effects on spontaneous locomotor activity in CD-1 mice. Compound **31** was devoid of any effects on distance moved over the dose range evaluated (10−150 mg/kg; Figure 5C). Together these *in vivo* data suggest that compound **31** ameliorates the phenotype of Kcnt1$^{L/L}$mice and may have an acceptable therapeutic window between efficacy (free brain concentration of 270 nM) and tolerability (maximum brain concentration 1204 nM at 150 mg/kg).

In conclusion, we have discovered a series of oxadiazole small molecule $K_{Na}1.1$ inhibitors that successfully demonstrate *in vivo* activity in a mouse model of *KCNT1* GoF. Future efforts will be aimed at evaluating the effects of longer-term

https://doi.org/10.1021/acsmedchemlett.0c00675
ACS Med. Chem. Lett. 2021, 12, 593−602

dosing on survival and behavior in the Kcnt1$^{L/L}$ mouse to better understand if the series holds therapeutic potential.

■ ASSOCIATED CONTENT

Supporting Information

The Supporting Information is available free of charge at https://pubs.acs.org/doi/10.1021/acsmedchemlett.0c00675.

Details of the chemical synthesis and characterization for compounds **3**, **4**, **27**, and **31**; ethical statement regarding the use of experimental animals in the studies; descriptions of the patch clamp procedure and the assays used to detect excitability; information regarding *in vitro* pharmacology testing of compound **31** in binding assays, with associated histogram (PDF)

■ AUTHOR INFORMATION

Corresponding Author

Andrew M. Griffin − *Praxis Precision Medicines, Research Innovation, Cambridge, Massachusetts 02142, United States*; Email: andrew@praxismedicines.com

Authors

Kristopher M. Kahlig − *Praxis Precision Medicines, Research Innovation, Cambridge, Massachusetts 02142, United States*

Robert John Hatch − *Praxis Precision Medicines, Research Innovation, Cambridge, Massachusetts 02142, United States; The Florey Institute of Neuroscience and Mental Health, Melbourne, VIC 3052, Australia*

Zoë A. Hughes − *Praxis Precision Medicines, Research Innovation, Cambridge, Massachusetts 02142, United States*

Mark L. Chapman − *ICAGEN, Durham, North Carolina 27703, United States*

Brett Antonio − *ICAGEN, Durham, North Carolina 27703, United States*

Brian E. Marron − *Praxis Precision Medicines, Research Innovation, Cambridge, Massachusetts 02142, United States*

Marion Wittmann − *Praxis Precision Medicines, Research Innovation, Cambridge, Massachusetts 02142, United States*

Gabriel Martinez-Botella − *Praxis Precision Medicines, Research Innovation, Cambridge, Massachusetts 02142, United States*

Complete contact information is available at: https://pubs.acs.org/10.1021/acsmedchemlett.0c00675

Author Contributions

The manuscript was written through contributions of all authors. All authors have given final approval to the final version of the manuscript.

Notes

The authors declare no competing financial interest.

■ ACKNOWLEDGMENTS

We thank Zhu Bai and the WuXi AppTech chemistry team for help with the compound syntheses discussed in this article as well as Rahul Nagawade and the chemistry team at Sai Life Sciences. We also thank Melody Li and Nikola Jancovski at The Florey Institute for performing the mouse *in vivo* EEG studies and Cristobal Alhambra for computational chemistry support provided for the HTS analysis. We also thank Kalpana Shankar at Simpson Healthcare for assistance with preparing the manuscript.

■ REFERENCES

(1) Kaczmarek, L. K. Slack, Slick and Sodium-Activated Potassium Channels. *ISRN Neurosci.* **2013**, *2013*, 354262.

(2) Smith, C. O.; Wang, Y. T.; Nadtochiy, S. M.; Miller, J. H.; Jonas, E. A.; Dirksen, R. T.; Nehrke, K.; Brookes, P. S. Cardiac metabolic effects of K(Na)1.2 channel deletion and evidence for its mitochondrial localization. *FASEB J.* **2018**, *32* (11), fj201800139R.

(3) Kim, G. E.; Kaczmarek, L. K. Emerging role of the KCNT1 Slack channel in intellectual disability. *Front. Cell. Neurosci.* **2014**, *8*, 209.

(4) Bhattacharjee, A.; Kaczmarek, L. K. For K+ channels, Na+ is the new Ca2+. *Trends Neurosci.* **2005**, *28* (8), 422−8.

(5) Spitznagel, B. D.; Mishra, N. M.; Qunies, A. M.; Prael, F. J., 3rd; Du, Y.; Kozek, K. A.; Lazarenko, R. M.; Denton, J. S.; Emmitte, K. A.; Weaver, C. D. VU0606170, a Selective Slack Channels Inhibitor, Decreases Calcium Oscillations in Cultured Cortical Neurons. *ACS Chem. Neurosci.* **2020**, *11* (21), 3658−3671.

(6) Pryce, K. D.; Powell, R.; Agwa, D.; Evely, K. M.; Sheehan, G. D.; Nip, A.; Tomasello, D. L.; Gururaj, S.; Bhattacharjee, A. Magi-1 scaffolds Na(V)1.8 and Slack K(Na) channels in dorsal root ganglion neurons regulating excitability and pain. *FASEB J.* **2019**, *33* (6), 7315−7330.

(7) Shore, A. N.; Colombo, S.; Tobin, W. F.; Petri, S.; Cullen, E. R.; Dominguez, S.; Bostick, C. D.; Beaumont, M. A.; Williams, D.; Khodagholy, D.; Yang, M.; Lutz, C. M.; Peng, Y.; Gelinas, J. N.; Goldstein, D. B.; Boland, M. J.; Frankel, W. N.; Weston, M. C. Reduced GABAergic Neuron Excitability, Altered Synaptic Connectivity, and Seizures in a KCNT1 Gain-of-Function Mouse Model of Childhood Epilepsy. *Cell Rep.* **2020**, *33* (4), 108303.

(8) Quraishi, I. H.; Stern, S.; Mangan, K. P.; Zhang, Y.; Ali, S. R.; Mercier, M. R.; Marchetto, M. C.; McLachlan, M. J.; Jones, E. M.; Gage, F. H.; Kaczmarek, L. K. An Epilepsy-Associated KCNT1Mutation Enhances Excitability of Human iPSC-Derived Neurons by Increasing Slack K(Na) Currents. *J. Neurosci.* **2019**, *39* (37), 7438−7449.

(9) Quraishi, I. H.; Mercier, M. R.; McClure, H.; Couture, R. L.; Schwartz, M. L.; Lukowski, R.; Ruth, P.; Kaczmarek, L. K. Impaired motor skill learning and altered seizure susceptibility in mice with loss or gain of function of the Kcnt1 gene encoding Slack (K(Na)1.1) Na(+)-activated K(+) channels. *Sci. Rep.* **2020**, *10* (1), 3213.

(10) Burbano, L. E.; Li, M.; Jancovski, N.; Jafar-Nejad, P.; Richards, K.; Sedo, A.; Soriano, A.; Rollo, B.; Jia, L.; Gazina, E.; Piltz, S.; Adikusuma, F.; Thomas, P. Q.; Rigo, F.; Reid, C. A.; Maljevic, S.; Petrou, S. Antisense oligonucleotide therapy for KCNT1 encephalopathy. *bioRxiv*, November 14, **2020**, ver. 1. DOI: 10.1101/2020.11.12.379164.

(11) Barcia, G.; Fleming, M. R.; Deligniere, A.; Gazula, V. R.; Brown, M. R.; Langouet, M.; Chen, H.; Kronengold, J.; Abhyankar, A.; Cilio, R.; Nitschke, P.; Kaminska, A.; Boddaert, N.; Casanova, J. L.; Desguerre, I.; Munnich, A.; Dulac, O.; Kaczmarek, L. K.; Colleaux, L.; Nabbout, R. De novo gain-of-function KCNT1 channel mutations cause malignant migrating partial seizures of infancy. *Nat. Genet.* **2012**, *44* (11), 1255−9.

(12) Rizzo, F.; Ambrosino, P.; Guacci, A.; Chetta, M.; Marchese, G.; Rocco, T.; Soldovieri, M. V.; Manocchio, L.; Mosca, I.; Casara, G.; Vecchi, M.; Taglialatela, M.; Coppola, G.; Weisz, A. Characterization of two de novoKCNT1 mutations in children with malignant migrating partial seizures in infancy. *Mol. Cell. Neurosci.* **2016**, *72*, 54−63.

(13) McTague, A.; Appleton, R.; Avula, S.; Cross, J. H.; King, M. D.; Jacques, T. S.; Bhate, S.; Cronin, A.; Curran, A.; Desurkar, A.; Farrell, M. A.; Hughes, E.; Jefferson, R.; Lascelles, K.; Livingston, J.; Meyer, E.; McLellan, A.; Poduri, A.; Scheffer, I. E.; Spinty, S.; Kurian, M. A.; Kneen, R. Migrating partial seizures of infancy: expansion of the electroclinical, radiological and pathological disease spectrum. *Brain* **2013**, *136* (5), 1578−1591.

(14) Derry, C. P.; Heron, S. E.; Phillips, F.; Howell, S.; MacMahon, J.; Phillips, H. A.; Duncan, J. S.; Mulley, J. C.; Berkovic, S. F.; Scheffer, I. E. Severe autosomal dominant nocturnal frontal lobe epilepsy

associated with psychiatric disorders and intellectual disability. *Epilepsia* **2008**, *49* (12), 2125−9.
(15) Lim, C. X.; Ricos, M. G.; Dibbens, L. M.; Heron, S. E. KCNT1 mutations in seizure disorders: the phenotypic spectrum and functional effects. *J. Med. Genet.* **2016**, *53* (4), 217−25.
(16) Heron, S. E.; Smith, K. R.; Bahlo, M.; Nobili, L.; Kahana, E.; Licchetta, L.; Oliver, K. L.; Mazarib, A.; Afawi, Z.; Korczyn, A.; Plazzi, G.; Petrou, S.; Berkovic, S. F.; Scheffer, I. E.; Dibbens, L. M. Missense mutations in the sodium-gated potassium channel gene KCNT1 cause severe autosomal dominant nocturnal frontal lobe epilepsy. *Nat. Genet.* **2012**, *44* (11), 1188−90.
(17) Pavone, P.; Polizzi, A.; Marino, S. D.; Corsello, G.; Falsaperla, R.; Marino, S.; Ruggieri, M. West syndrome: a comprehensive review. *Neurol. Sci.* **2020**, *41*, 3547.
(18) Hrachovy, R. A.; Frost, J. D., Jr. Infantile spasms. *Handb Clin Neurol* **2013**, *111*, 611−8.
(19) Ohtahara, S.; Yamatogi, Y. Ohtahara syndrome: with special reference to its developmental aspects for differentiating from early myoclonic encephalopathy. *Epilepsy Res.* **2006**, *70* (Suppl 1), S58−67.
(20) Gertler, T.; Bearden, D.; Bhattacharjee, A.; Carvill, G. KCNT1-Related Epilepsy. In *GeneReviews*; Adam, M. P., Ardinger, H. H., Pagon, R. A., Wallace, S. E., Bean, L. J. H., Stephens, K., Amemiya, A., Eds.; University of Washington: Seattle, WA, 1993.
(21) Gertler, T. S.; Thompson, C. H.; Vanoye, C. G.; Millichap, J. J.; George, A. L., Jr. Functional consequences of a KCNT1 variant associated with status dystonicus and early-onset infantile encephalopathy. *Ann. Clin. Transl. Neurol.* **2019**, *6* (9), 1606−1615.
(22) Cole, B. A.; Johnson, R. M.; Dejakaisaya, H.; Pilati, N.; Fishwick, C. W. G.; Muench, S. P.; Lippiat, J. D. Structure-Based Identification and Characterization of Inhibitors of the Epilepsy-Associated K(Na)1.1 (KCNT1) Potassium Channel. *iScience* **2020**, *23* (5), 101100.
(23) de Los Angeles Tejada, M.; Stolpe, K.; Meinild, A. K.; Klaerke, D. A. Clofilium inhibits Slick and Slack potassium channels. *Biologics* **2012**, *6*, 465−70.
(24) Bearden, D.; Strong, A.; Ehnot, J.; DiGiovine, M.; Dlugos, D.; Goldberg, E. M. Targeted treatment of migrating partial seizures of infancy with quinidine. *Ann. Neurol.* **2014**, *76* (3), 457−61.
(25) Yang, B.; Gribkoff, V. K.; Pan, J.; Damagnez, V.; Dworetzky, S. I.; Boissard, C. G.; Bhattacharjee, A.; Yan, Y.; Sigworth, F. J.; Kaczmarek, L. K. Pharmacological activation and inhibition of Slack (Slo2.2) channels. *Neuropharmacology* **2006**, *51* (4), 896−906.
(26) Mullen, S. A.; Carney, P. W.; Roten, A.; Ching, M.; Lightfoot, P. A.; Churilov, L.; Nair, U.; Li, M.; Berkovic, S. F.; Petrou, S.; Scheffer, I. E. Precision therapy for epilepsy due to KCNT1 mutations. A randomized trial of oral quinidine. *Neurology* **2018**, *90* (1), e67−e72.
(27) Fitzgerald, M. P.; Fiannacca, M.; Smith, D. M.; Gertler, T. S.; Gunning, B.; Syrbe, S.; Verbeek, N.; Stamberger, H.; Weckhuysen, S.; Ceulemans, B.; Schoonjans, A.-S.; Rossi, M.; Demarquay, G.; Lesca, G.; Olofsson, K.; Koolen, D. A.; Hornemann, F.; Baulac, S.; Rubboli, G.; Minks, K. Q.; Lee, B.; Helbig, I.; Dlugos, D.; Møller, R. S.; Bearden, D. Treatment Responsiveness in KCNT1-Related Epilepsy. *Neurotherapeutics* **2019**, *16* (3), 848−857.
(28) Martinez, B. G.; Griffin, A.; Charifson, P.; Reddy, K.; Kahlig, M. K.; Marron, B., Kcnt1 Inhibitors And Methods Of Use. Patent WO/2020/227101, November 12, 2020.
(29) Sheets, P. L.; Heers, C.; Stoehr, T.; Cummins, T. R. Differential block of sensory neuronal voltage-gated sodium channels by lacosamide [(2R)-2-(acetylamino)-N-benzyl-3-methoxypropanamide], lidocaine, and carbamazepine. *J. Pharmacol. Exp. Ther.* **2008**, *326* (1), 89−99.
(30) Willow, M.; Gonoi, T.; Catterall, W. A. Voltage clamp analysis of the inhibitory actions of diphenylhydantoin and carbamazepine on voltage-sensitive sodium channels in enrupblastoma cells. *Mol. Pharmacol.* **1985**, *27* (5), 549−558.
(31) Rogawski, M. A.; Löscher, W.; Rho, J. M. Mechanisms of action of antiseizure drugs and the ketogenic diet. *Cold Spring Harbor Perspect. Med.* **2016**, *6* (5), a022780.

NOTE ADDED AFTER ASAP PUBLICATION

This letter published ASAP on March 9, 2021, with an error in Figure 2. The corrected version was reposted on March 29, 2021.

https://doi.org/10.1021/acsmedchemlett.0c00675
ACS Med. Chem. Lett. 2021, 12, 593−602